Information Support of Optimization Calculation of Vortex Type Granulation Devices

Artem Artyukhov(✉)

Sumy State University, 2 Rymskogo-Korsakova St., Sumy 40007, Ukraine
artyukhov@pohnp.sumdu.edu.ua

Abstract. The paper studies the hydrodynamic conditions of gas flow motion and vortex granulator workspace design optimization. A comprehensive approach for determination of the hydrodynamic characteristics of a vortex gas flow and their visualization is proposed. The mathematical approach, based on Reynolds equations for turbulent flows solution, is presented. The mathematical model of equations solution with the definition of gas flow velocity components in any point on the radius and height of vortex granulator is obtained. The value of gas flow components of velocity, received by the results of analytical solution, and experimental data has a high degree of compliance. There is mutual rejection that numerical value of velocities and overall graphic image of diagrams of components of gas flow velocities have the same character. For rate and radial velocity components of gas flow for the initial conditions and changing set of geometrical and technological conditions does not cause such significant change of quantitative distribution value along the radius and height for angular velocity component gas stream. The obtained results form the basis of original algorithm for calculating of vortex granulator hydrodynamic calculation and its basic dimensions optimization selection.

Keywords: Software · Modeling · Vortex granulator · Hydrodynamics Optimization

1 Introduction

Flows of single-phase and multiphase medium play a key role in the working process of many contemporary engineering devices. The design of these devices for the required operating parameters is impossible without a reliable prediction of the characteristics of these flows. Since many modern engineering devices are expensive and time consuming to manufacture, physical modeling with the experimental determination of the parameters of their work in different modes, as a rule, requires a lot of time and cost. In addition, because of limited possibilities of modern experimental sensors and measuring instruments, experimental observations do not provide a complete picture of the phenomenon being investigated.

V. Ivanov et al. (Eds.): DSMIE 2018, LNME, pp. 412–421, 2019.
https://doi.org/10.1007/978-3-319-93587-4_43

2 Literature Review

Because of nature of these environments, flow of liquids and gases often varies in complex manner to form nonstationary effects, “dead” zones and vortex structures [1]. The situation is further complicated by the presence of heat transfer, in considering flows of several substances mixture, flows with free surfaces, weighted particles in stream, flows with cavitation, boiling, condensation, combustion, chemical reactions [2–8]. These factors lead to the growing interest of mathematical modeling tools for flows of liquids and gases, which allows to predict the flow characteristics and parameters of the devices at design stages and stages of manufacturing in the metal [9–12].

Software can adequately simulate the complex physical effects taking place in flows motion in vortex granulator, and perform calculation of flows within the reasonable time [13, 14]. They provide the user with the convenient tools of data preparation and analysis of calculations results, and are a powerful tool for accurate prediction of the characteristics of hydraulic parts flow at a design stage, saving the resources to conduct a physical experiment [15, 16].

Methods CFD (Computational Fluid Dynamics) suggest calculation of flows of liquids and gases through the numerical solution of equations of Navier-Stokes and continuity, describing the most general case of this medium motion (for turbulent flows - Reynolds equations).

The purpose of the work is creation of vortex granulator optimization calculation algorithm. The created algorithm is based on the author’s software and calculation data visualization using software for calculation of flows hydrodynamics.

3 Research Methodology

The simulation of flows is based on the finite-volume method of solving equations of hydrodynamics and the use of a rectangular adaptive grid with local grinding. For the approximation of the curvilinear geometry with increased accuracy, the technology of the substrate density of geometry is used. This technology allows importing geometry from CAD systems and transferring information with finite element analysis systems.

Given that, in practice interest it usually deals with not instantaneous, but with the average in time velocity value, for mathematical description of turbulent swirling motion of gas flow Reynolds equation as modification of Navier-Stokes equations is used [17, 18].

$$\frac{\partial}{\partial t}\left(\rho\overline{V_i}\right) + \frac{\partial}{\partial q_j}\left(\rho\overline{V_i V_j}\right) + \frac{\partial}{\partial q_j}\left(\rho\overline{V_i' V_j}\right) = -\frac{\partial p}{\partial q_i} + \frac{\partial}{\partial q_j}\left[\mu\left(\frac{\partial\overline{V_i}}{\partial q_j} + \frac{\partial\overline{V_j}}{\partial q_i}\right)\right] + f_i \quad (1)$$

where $\bar{V}$- average in time values of velocity; $\bar{V}'$- components of velocity pulsations; μ - coefficient of turbulent viscosity; t - time; ρ - gas density; p - pressure; f_i – element, characterizing the mass forces effect; q_j - coordinate axes (in the case of hydrodynamic modeling in granulator working volume as it is shown above, it is advisable to use curvilinear coordinate system), i, j − 1 … 3; for cylindrical coordinate system (Fig. 1) code "1" – axial direction (z), code "2" – radial direction (r), code "3" – circular direction (φ) (Figs. 1 and 2).

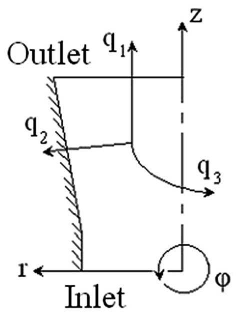

Fig. 1. Scheme of vortex granulator workspace and coordinate system.

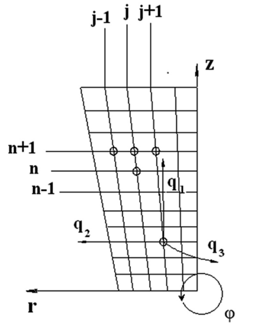

Fig. 2. Construction of calculation grid.

The main advantages of description and problem solving hydrodynamics method, based on numerical solution of Reynolds complete equations, are accuracy and versatility.

The Reynolds equations system is supplemented with flow continuity equation

$$\frac{\partial \rho}{\partial t} + \frac{\partial}{\partial q_j}\left(\rho V_j\right) = 0. \tag{2}$$

For Reynolds Eq. (1) solving Boussinesq hypothesis [17] is used. According to this hypothesis, the members with velocity pulsations $\left(\rho \overline{V_i' V_j'}\right)$ in Eq. (3) are associated with the averaged flow characteristics in such relation:

$$\rho \overline{V_i' V_j'} = -\mu \left(\frac{\partial \overline{V_i}}{\partial q_j} + \frac{\partial \overline{V_j}}{\partial q_i} \right) + \frac{2}{3} \rho \delta_{ij} k, \tag{3}$$

where $k = 0,5\left(\overline{V_j' V_j'}\right)$ – turbulence kinetic energy, δij = 1 when i = j, δi = 0 when i $\neq$ j.

The Reynolds system of equations is elliptic. It is used to calculate the trends in those cases where flow characteristics at arbitrary point area depend on the structure of flow both above and downstream, i.e. when the dominant direction of the fluid is absent or weakly expressed. Ellipticity system of equations means that it is necessary to set the boundary conditions for all variables in all the borders of calculation area.

When axisymmetrical flow modeling equation of motion (1) and continuity of flow (2) are significantly simplified. For curved (cylindrical) coordinate system they are as follows (with the introduction of Eq. (3) Reynolds number Re = V_0D/ν where characteristic parameters D – diameter of input cross section calculation area; V_0 - average rate velocity in the input section; ν - kinematic viscosity):

– Reynolds equations projected on the axial direction q1:

$$\begin{aligned}
&\frac{V_1}{H_1}\frac{\partial V_1}{\partial q_1}+\frac{V_2}{H_2}\frac{\partial V_1}{\partial q_2}-\frac{V_2^2}{H_1H_2}\frac{\partial H_2}{\partial q_1}-\frac{V_3^2}{H_1H_3}\frac{\partial H_3}{\partial q_1}+\frac{1}{H_2}\frac{\partial\left(\overline{V_1'V_2'}\right)}{\partial q_2}+\frac{\left(\overline{V_1'V_2'}\right)}{H_1^2H_2H_3}\frac{\partial\left(H_1^2H_3\right)}{\partial q_2}\\
&+\frac{1}{H_1}\frac{\partial\left(\overline{V_1'V_1'}\right)}{\partial q_1}+\frac{\left(\overline{V_1'V_1'}\right)}{H_1^2H_2H_3}\frac{\partial(H_1H_2H_3)}{\partial q_1}-\frac{\left(\overline{V_2'V_2'}\right)}{H_1H_2}\frac{\partial H_2}{\partial q_1}-\frac{\left(\overline{V_3'V_3'}\right)}{H_1H_3}\frac{\partial H_3}{\partial q_1}=-\frac{1}{H_1}\frac{\partial p}{\partial q_1}\\
&+\frac{1}{\mathrm{Re}}\left(\frac{1}{H_1^2}\frac{\partial^2V_1}{\partial q_1^2}+\frac{1}{H_2^2}\frac{\partial^2V_1}{\partial q_2^2}+\frac{1}{H_1H_2H_3}\frac{\partial V_1}{\partial q_1}\frac{\partial(H_2H_3/H_1)}{\partial q_1}+\frac{1}{H_1H_2H_3}\frac{\partial V_1}{\partial q_2}\frac{\partial(H_1H_3/H_2)}{\partial q_2}\right.\\
&-\frac{2}{H_1H_2^2}\frac{\partial H_2}{\partial q_1}\frac{\partial V_2}{\partial q_2}+\frac{V_1}{H_1}\frac{\partial}{\partial q_1}\left(\frac{1}{H_1H_2H_3}\frac{\partial(H_2H_3)}{\partial q_1}\right)\\
&\left.+\frac{V_2}{H_1}\frac{\partial}{\partial q_1}\left(\frac{1}{H_1H_2H_3}\frac{\partial(H_1H_3)}{\partial q_2}\right)-\frac{V_2}{H_2H_3}\frac{\partial}{\partial q_2}\left(\frac{H_3}{H_1H_2}\frac{\partial H_2}{\partial q_1}\right)\right);
\end{aligned}\tag{4}$$

– Reynolds equations projected on the radial direction q2:

$$\begin{aligned}
&\frac{V_1}{H_1}\frac{\partial V_2}{\partial q_1}+\frac{V_2}{H_2}\frac{\partial V_2}{\partial q_2}-\frac{V_1V_2}{H_1H_2}\frac{\partial H_2}{\partial q_1}-\frac{V_3^2}{H_2H_3}\frac{\partial H_3}{\partial q_2}+\frac{1}{H_1}\frac{\partial\left(\overline{V_1'V_2'}\right)}{\partial q_1}+\frac{\left(\overline{V_1'V_2'}\right)}{H_1H_2^2H_3}\frac{\partial\left(H_2^2H_3\right)}{\partial q_1}\\
&+\frac{1}{H_2}\frac{\partial\left(\overline{V_2'V_2'}\right)}{\partial q_2}+\frac{\left(\overline{V_2'V_2'}\right)}{H_1H_2^2H_3}\frac{\partial(H_1H_2H_3)}{\partial q_2}-\frac{\left(\overline{V_3'V_3'}\right)}{H_2H_3}\frac{\partial H_3}{\partial q_2}=-\frac{1}{H_2}\frac{\partial p}{\partial q_2}\\
&+\frac{1}{\mathrm{Re}}\left(\frac{1}{H_1^2}\frac{\partial^2V_2}{\partial q_1^2}+\frac{1}{H_2^2}\frac{\partial^2V_2}{\partial q_2^2}+\frac{1}{H_1H_2H_3}\frac{\partial V_2}{\partial q_1}\frac{\partial(H_2H_3/H_1)}{\partial q_1}+\frac{1}{H_1H_2H_3}\frac{\partial V_2}{\partial q_2}\frac{\partial(H_1H_3/H_2)}{\partial q_2}\right.\\
&\left.+\frac{2}{H_1H_2^2}\frac{\partial H_2}{\partial q_1}\frac{\partial V_1}{\partial q_2}+\frac{V_2}{H_2}\frac{\partial}{\partial q_2}\left(\frac{1}{H_1H_2H_3}\frac{\partial(H_1H_3)}{\partial q_2}\right)\right);
\end{aligned}\tag{5}$$

– Reynolds equations projected on the circular direction q3:

$$\begin{aligned}
&\frac{V_1}{H_1}\frac{\partial V_3}{\partial q_1}+\frac{V_2}{H_2}\frac{\partial V_3}{\partial q_2}+\frac{V_1V_3}{H_1H_3}\frac{\partial H_3}{\partial q_1}+\frac{V_2V_3}{H_2H_3}\frac{\partial H_3}{\partial q_2}+\frac{1}{H_2}\frac{\partial\left(\overline{V_2'V_3'}\right)}{\partial q_2}+\frac{\left(\overline{V_2'V_3'}\right)}{H_1H_2H_3^2}\frac{\partial\left(H_1H_3^2\right)}{\partial q_2}\\
&+\frac{1}{H_1}\frac{\partial\left(\overline{V_1'V_3'}\right)}{\partial q_1}+\frac{\left(\overline{V_1'V_3'}\right)}{H_1H_2H_3^2}\frac{\partial\left(H_2H_3^2\right)}{\partial q_1}=\frac{1}{\mathrm{Re}}\left(\frac{1}{H_1^2}\frac{\partial^2V_3}{\partial q_1^2}+\frac{1}{H_2^2}\frac{\partial^2V_3}{\partial q_2^2}\right.\\
&\left.+\frac{1}{H_1H_2H_3}\frac{\partial V_3}{\partial q_1}\frac{\partial(H_2H_3/H_1)}{\partial q_1}+\frac{1}{H_1H_2H_3}\frac{\partial V_3}{\partial q_2}\frac{\partial(H_1H_3/H_2)}{\partial q_2}+\frac{V_3}{H_1H_2}\frac{\partial}{\partial q_2}\left(\frac{H_1}{H_2H_3}\frac{\partial H_3}{\partial q_2}\right)\right);
\end{aligned}\tag{6}$$

– continuity equation:

$$\frac{1}{H_1H_2H_3}\left(V_1\frac{\partial(H_2H_3)}{\partial q_1}+V_2\frac{\partial(H_3H_1)}{\partial q_2}\right)+\frac{1}{H_1}\frac{\partial V_1}{\partial q_1}+\frac{1}{H_2}\frac{\partial V_2}{\partial q_2}=0,\tag{7}$$

where H1, H2, H3 – Lamé coefficient [17].

Further simplification of system of Eqs. (4)–(7) for simulating the vortex flow of gas phase in the workspace granulator is possible using the following assumptions [19, 20]:

- the expected presence of dominant flow direction along with the axial component of gas flow velocity is everywhere positive and far exceeds the radial;
- gas flow velocity component in the axial direction varies considerably slower than in the radial;
- velocity and pressure values in every elementary volume of gas flow depend only on the conditions downstream and do not depend on the conditions upstream.

These assumptions allow to conduct analysis of components in Eqs. (4)–(7) and discard those that provide significant impact on the result of the calculation.

After accounting assumptions for axially symmetric gas flow Eq. (4)–(7) can be written as

$$\begin{aligned}\frac{V_1}{H_1}\frac{\partial V_1}{\partial q_1}+\frac{V_2}{H_2}\frac{\partial V_1}{\partial q_2}-\frac{V_3^2}{H_1H_3}\frac{\partial H_3}{\partial q_1}+\frac{1}{H_2}\frac{\partial\left(\overline{V_1'V_2'}\right)}{\partial q_2}+\frac{\left(\overline{V_1'V_2'}\right)}{H_1^2H_2H_3}\frac{\partial\left(H_1^2H_3\right)}{\partial q_2}\\ =-\frac{1}{H_1}\frac{\partial p}{\partial q_1}+\frac{1}{\mathrm{Re}}\left(\frac{1}{H_2^2}\frac{\partial^2V_1}{\partial q_2^2}+\frac{1}{H_1H_2H_3}\frac{\partial V_1}{\partial q_2}\frac{\partial(H_1H_3/H_2)}{\partial q_2}\right);\end{aligned} \tag{8}$$

$$\frac{\partial p_r}{\partial q_2}=\frac{V_3^2}{H_3}\frac{\partial H_3}{\partial q_2}; \tag{9}$$

$$\begin{aligned}\frac{V_1}{H_1}\frac{\partial V_3}{\partial q_1}+\frac{V_2}{H_2}\frac{\partial V_3}{\partial q_2}+\frac{V_1V_3}{H_1H_3}\frac{\partial H_3}{\partial q_1}+\frac{V_2V_3}{H_2H_3}\frac{\partial H_3}{\partial q_2}+\frac{1}{H_2}\frac{\partial(\overline{V_2'V_3'})}{\partial q_2}+\frac{(\overline{V_2'V_3'})}{H_1H_2H_3^2}\frac{\partial(H_1H_3^2)}{\partial q_2}\\ =\frac{1}{\mathrm{Re}}\left(\frac{1}{H_2^2}\frac{\partial^2V_3}{\partial q_2^2}+\frac{1}{H_1H_2H_3}\frac{\partial V_3}{\partial q_2}\frac{\partial(H_1H_3/H_2)}{\partial q_2}+\frac{V_3}{H_1H_2}\frac{\partial}{\partial q_2}\left(\frac{H_1}{H_2H_3}\frac{\partial H_3}{\partial q_2}\right)\right);\end{aligned} \tag{10}$$

$$\frac{1}{H_1H_2H_3}\left(V_1\frac{\partial(H_2H_3)}{\partial q_1}+V_2\frac{\partial(H_3H_1)}{\partial q_2}\right)+\frac{1}{H_1}\frac{\partial V_1}{\partial q_1}+\frac{1}{H_2}\frac{\partial V_2}{\partial q_2}=0. \tag{11}$$

This system of equations is closed equation sustainability costs:

$$\int_0^{Q_2}V_1H_2H_3dq_2=const, \tag{12}$$

where Q2 - coordinate q2 on the wall of working volume of vortex granulator.

Obtained system of Eqs. (8)–(11) has a parabolic character, and its decision based on the method proposed by Patankar and Spalding [20] and realized in SIMPLE (Semi-Implicit Method for Pressure-Linked Equations) procedure and its modifications.

Numerical solutions of mathematical models equations are performed in one marching passage from the working volume input cross section to output using finite volumes method with the elements of finite-element approach. Before calculating the estimated grid is constructed (Fig. 2), and unknown values of velocity and pressure are found in the nodes of this grid.

The program «Conical channel» © is designed to calculate axial symmetric gas flows in channels, including the swirling flows in the diffuser on the base of the model [21].

Initial data for calculation are geometric configuration of channel properties and parameters of gas and parameters of flow in the input cross-section. The calculation objective is to determine the fields of velocity and pressure in full range of calculated area and, consequently, the determination of energy losses between the input and output cross sections of the channel. The program displays the calculation data as graphic dependencies.

Program's work starts with opening or creating a new file of calculated area configuration. Example of calculation area configuration is shown in Fig. 3.

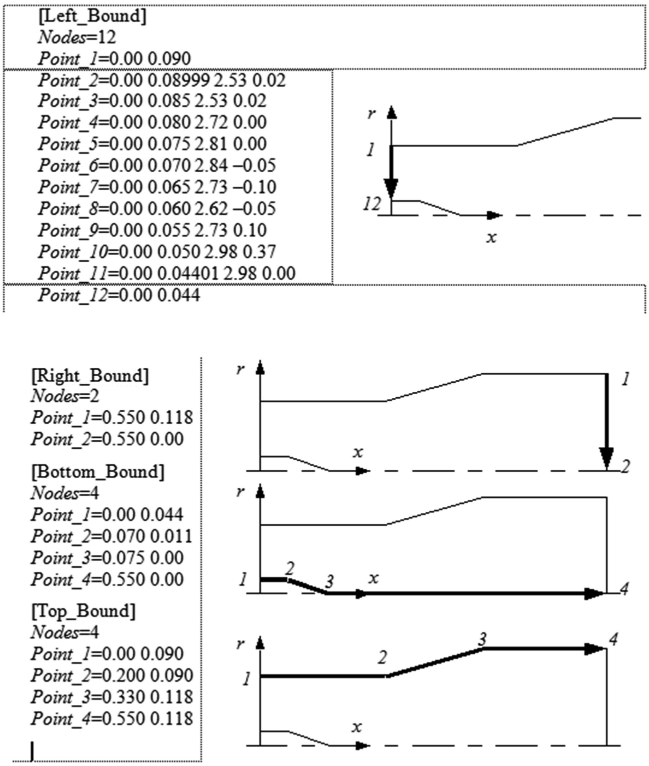

Fig. 3. Example of calculation area configuration.

After selecting the necessary parameter for calculation the program «Conical channel» © builds an estimated grid (Fig. 2).

4 Results

For the analysis of motion velocity components it is necessary to define the nature of dependencies of the graphical components and match them within a comparative graph as it is shown in Figs. 4, 5, 6.

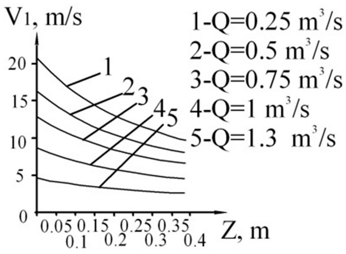

Fig. 4. Calculated change of the longitudinal velocity of the gas flow.

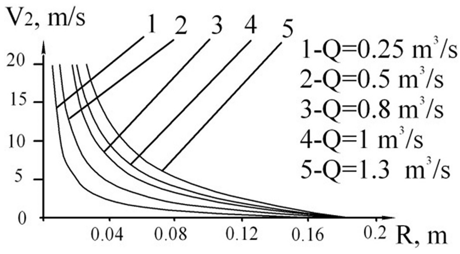

Fig. 5. Calculated change of the radial velocity of the gas flow.

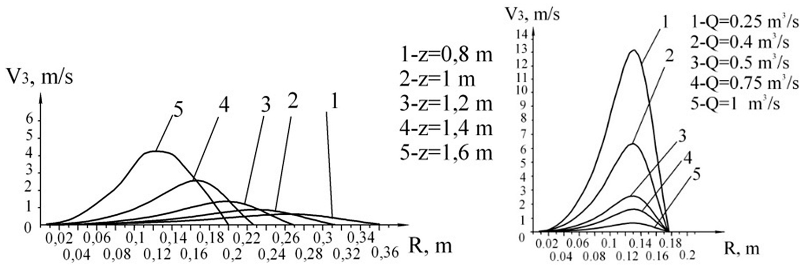

Fig. 6. Calculated change of the circumferential velocity of the gas flow.

Analysis of graphic dependences of gas flow rate velocity under various conditions has identified monotonous nature of rate velocity reduction under all calculations of the conducting conditions.

Comparison of theoretical calculation for different cross sections of working space and different opening cone angles shows that the area of maximum circular speed for the arbitrarily chosen section is r = 0.66–0.72 R.

Analysis of graphical dependencies shows the reduction zone of circular velocity growth by increasing the gas flow rate and narrowing the range of maximum speed. This velocity peak remains constant at geometric place in the working space of vortex granulator.

The value of circular velocity with increasing the gas flow rate increases faster. At the same time, with the increasing gas flow rate in the workspace of vortex granulator the angular velocity slow growth zone is growing. Thus, the vortex is moving toward the solid wall and has a greater intensity.

Analysis of dependences of circular velocity changes under different conditions identified pattern of velocity distribution by the radius of device and its quality change according to the set of parameters.

Given the results of analysis of circular velocity peak of gas flow in cross section of the device workspace for the granular product from the melt (solution) device (or group of devices) for spraying it is advisable to locate within the working space of vortex granulator in specified range of current radius at random selected height and cone opening angle the received results of experiment (optimal height of location sprayer is defined to be h = 0.6–0.8 H).

Continuous increase of the circular velocity of gas flow before reaching its peak and reduction after passing its peak had obtained confirmation by the experiment and defined the range of gas distribution unit operation with maximum efficiency. In the area of minimum circular velocity the granules motion intensification and “dead” zones prevention, that is possible in the range up to r = 0.25 R, are achieved by reasonable selection of gas-distributing unit with additional elements for flow swirling.

According to the analysis the influence of conical workspace opening angle on the possibility of reverse vortex in the center of a weighted layer and place a geometric location of individual elements of the weighted layer connection place and the transition region combining the weighted layer connection was identified. With the

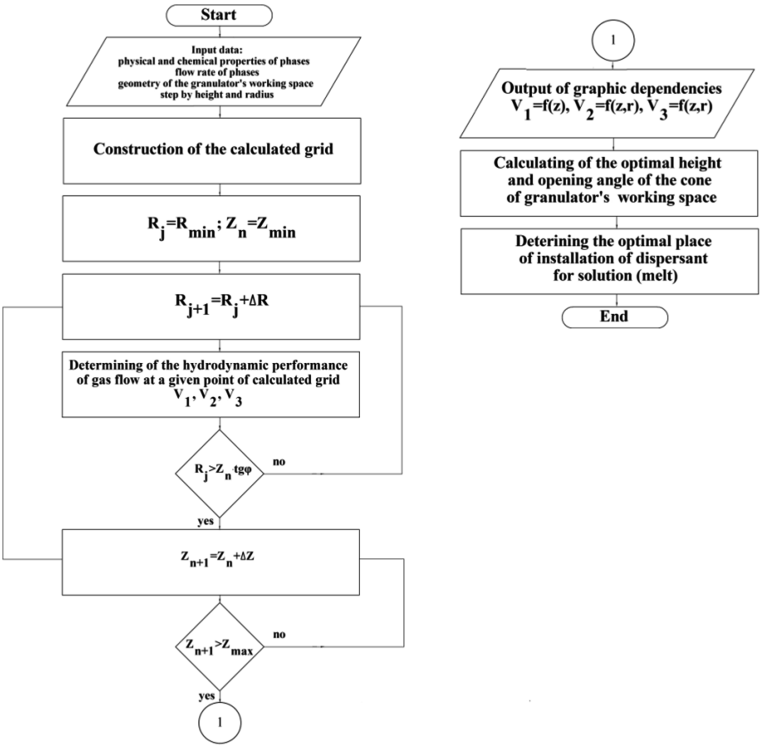

Fig. 7. An algorithm for vortex granulator hydrodynamic calculating.

increasing of cone opening angle (up to 10–13°) zone of reverse vortex has a constant value and is determined within r = (0.15–0.25) R. This situation is observed before h = (0.3–0.4) H. Recirculation zone is located in the inlet of diffuser.

Based on the analysis of hydrodynamic properties of gas flow due to certain variables the rational selection of geometry workspace vortex granulator becomes possible (opening angle α and height z).

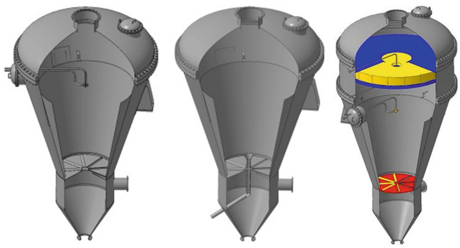

a b c

Fig. 8. Vortex granulator designs: a – with spraying of the melt; b – with a previous wetting of granules and simple inner case; c – with separating device for exhaust gases cleaning.

5 Conclusions

Simulation results allowed us to develop an algorithm for vortex granulator hydrodynamic calculating, which is represented on Fig. 7.

Example of granulator design based on hydrodynamic calculation (porous ammonium nitrate production, final product performance 3000 kg/day, commodity fraction – granules 2–3 mm) is shown in Fig. 8.

Acknowledgements. This work was carried out under the project « Improving the efficiency of granulators and dryers with active hydrodynamic regimes for obtaining, modification and encapsulation of fertilizers» , state registration No. 0116U006812. While preparing the article the information about the original designs of vortex granulators (Patents Nos. 99023 Ukraine IPC (2012.01) B01J2/16, Ukraine IPC 110992 B01J2/00, B01J2/16, 111406 Ukraine IPC B01J2/04, B01J2/16 etc.) and the author's software product were used (certificate of authorship No. 67472). The authors thank the researchers of Processes and Equipment of Chemical and Refining Industries Department, Sumy State University, for their valuable comments during the article preparation.

References

1. Artyukhov, A.E., Sklabinskyi, V.I.: Experimental and industrial implementation of porous ammonium nitrate producing process in vortex granulators. Naukovyi Visnyk Natsionalnoho Hirnychoho Universytetu **6**, 42–48 (2013)
2. Ashcraft, R., Heynderickx, G., Marin, G.: Modeling fast biomass pyrolysis in a gas-solid vortex reactor. Chem. Eng. J. **207–208**, 195–208 (2012)

3. Khalatov, A.: Heat transfer and hydrodynamics in the fields of mass forces. J. Eng. Phys. Thermophys. **83**(4), 794–808 (2010)
4. Kaewklum, R., Kuprianov, V., Douglas, P.: Hydrodynamics of air-sand flow in a conical swirling fluidized bed: A comparative study between tangential and axial air entries. Energy Convers. Manag. **50**, 2999–3006 (2009)
5. Volchkov, E., Dvornikov, N., Lukashov, V., Abdrakhmanov, R.: Investigation of the flow in the vortex chamber with centrifugal fluidizing bed with and without combustion. Thermophys. Aeromech. **20**(6), 663–668 (2013)
6. Shi, D.-P., Luo, Z.H., Guo, A.Y.: Numerical Simulation of the gas – solid flow in fluidized-bed polymerization reactors. Ind. Eng. Chem. Res. **49**(9), 4070–4079 (2010)
7. Pandaba, P., Sukanta, K.D.: Numerical simulation for hydrodynamic analysis and pressure drop prediction in horizontal gas-solid flows. Part. Sci. Technol. **32**(1), 94–103 (2014)
8. Feldmann, F., Hagemann, B., Ganzer, L., Panfilov, M.: Numerical simulation of hydrodynamic and gas mixing processes in underground hydrogen storages. Environ. Earth Sci. **75**, 1165–1172 (2016)
9. Kwauk, M.: Fluidization: Idealized and Bubbleless, with Application. Science Press, Beijing (1992)
10. Gidaspow, D.: Multiphase Flow and Fluidization: Continuum and Kinetic Theory Descriptions with Applications. Academic Press, San Diego (1994)
11. Salman, A., Hounslow, M., Seville, J.: Granulation. Elsevier Science, London (2006)
12. Yang, W.: Handbook of Fluidizaition and fluid-Particle Systems. Marcel Dekker, New York (2003)
13. Artyukhov, A.E., Fursa, A.S., Moskalenko, K.V.: Classification and separation of granules in vortex granulators. Chem. Pet. Eng. **51**(5–6), 311–318 (2015)
14. Crowe, C.: Multiphase Flow Handbook. Taylor & Francis Group, Boca Raton (2006)
15. Dvornikov, N., Belousov, P.: Investigation of a fluidized bed in a vortex chamber. J. Appl. Mech. Tech. Phys. **52**(2), 206–211 (2011)
16. Caiyuan, Y., Tao, Q., Xizhong, W.: Heat and mass transfer in process of fluidized bed spray granulation. Chin. J. Chem. Eng. **16**(6), 836–839 (2004)
17. Sinaiski, E.G.: Hydromechanics: Theory and Fundamentals. Wiley-VCH Verlag GmbH & Co. KGaA, Weinheim (2010)
18. Tenneti, S., Subramaniam, S.: Particle-resolved direct numerical simulation for gas-solid flow model development. Annu. Rev. Fluid Mech. **46**, 199–230 (2014)
19. Yang, J., Wang, Q., Zeng, M., Nakayama, A.: Computational study of forced convective heat transfer in structured packed beds with spherical or ellipsoidal particles. Chem. Eng. Sci. **65**(2), 726–738 (2010)
20. Patankar, S.V.: Numerical Heat Transfer and Fluid Flow. Hemisphere Publishing Corp, Washington (1980)
21. Artyukhov, A., Sklabinskyi, V.: Theoretical analysis of granules movement hydrodynamics in the vortex granulators of ammonium nitrate and carbamide production. Chem. Chem. Technol. **9**(2), 175–180 (2015)